ATLAS Internal Note
INDET-NO-110
4 Sep. 1995

Performance Studies for the Atlas Inner Detector SCT at r = 30 cm with Strips and Large Pixels

C. Geich-Gimbel[a], P. Luthaus[b], C. Linder[c], T. Maron[c], S. Menke[a], M. Pingel[b], G. Stavropoulos[b]

[a] Physikalisches Institut, Universität Bonn, FRG
[b] Experimentelle Physik IV, Universität Dortmund, FRG
[c] Fachbereich Physik, Bergische Universität, Wuppertal, FRG

1) Introduction

In this note various aspects of the performance of the Atlas[1][2] inner detector barrel are given for two alternative layouts: crossed strips ("X-ST"; sometimes called small angle stereo strips, too) or large pixels ("LPIX"), respectively, at a radius of 30 cm. The geometrical specifications are outlined below.

We include calculations as well as Monte Carlo studies concerning the occupancy of these detector elements at the full LHC luminosity. Occupancies and possible ambiguities due to ghost hits for the case of intersecting strips might be of major importance.

2) Definition of geometries

Each SCT layer consists of several equally shaped sublayers. In z-direction each sublayer is divided into seven modules with two active planes of $6 \times 12\,\mathrm{cm}^2$. The active planes are made of silicon strip detectors with 800 $12\,\mathrm{cm} \times 75\,\mu\mathrm{m}$ strips each. A crossing angle of 40 mrad between the two detector layers leads to an effective pixel size of

$$F_{\mathrm{eff}} = 75\,\mu\mathrm{m}\frac{75\,\mu\mathrm{m}}{\sin(40\,\mathrm{mrad})} \simeq 75\,\mu\mathrm{m} \times 2\,\mathrm{mm} \quad ,$$

which is 3/4 of the size of the large pixel cells, which, in turn, have a size of $100\,\mu\mathrm{m} \times 2\,\mathrm{mm}$ (see fig. 1). Each single u-strip is crossed by 64 adjacent v-strips.

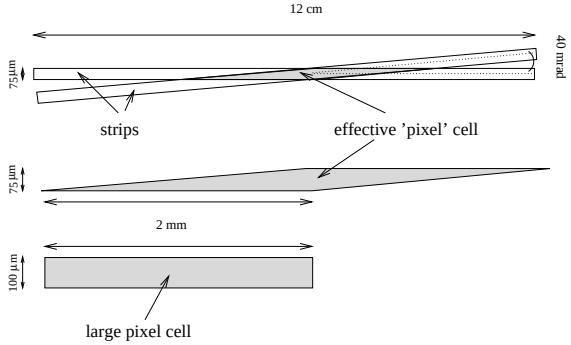

Figure 1: Comparison of the effective pixel size of two crossed strips with a large pixel cell.

3) Track parameter resolution
The following results are based on samples of 1000 tracks each, generated from SLUG/DICE[3][4], for electrons and muons, at four different momenta (10, 50, 100 and 500 GeV), in an η-range of ± 0.5 (full ϕ-range), for two layouts: (a) the present SCT, (b) replacing the inner layer at $r = 30\,\mathrm{cm}$ by a large pixel layer.
The pattern recognition scheme used is based on iPatRec[5] and the DICE geometry adapted for large pixel layers at $r = 30\,\mathrm{cm}$ [6].

Some figures of merit are given in table 1. Sigma-values from Gaussian fits to the difference between true and reconstructed quantities are given throughout, comparing generated tracks and reconstructed ones as obtained by the so-called vertex-fit. The errors (not given explicitly) amount to 3% of the values given, unless for electrons at 500 GeV, where the width of the p_T-ratio has an uncertainty of 7.9%. A typical distribution is shown in fig. 2.

Concerning a_0, the transverse impact parameter, values of about 7 μm are obtained; for the longitudinal vertex position, z_0, we get 5 cm.

3.1) Conclusion from track parameters
In a very brief conclusion, the resolutions obtained for track parameters are quite similar in both layouts.
This result is expected: With reference to the geometrical specifications outlined above, one obtains the following r.m.s. in the z-direction: $1/\sqrt{12} \times 2000\mu\mathrm{m} = 577\mu\mathrm{m}$ for the large pixels (rectangular distribution), and $1/\sqrt{24} \times 4000\mu\mathrm{m} = 816\mu\mathrm{m}$ (triangular distribution) for crossing strips, demanding coincident hits in both layers. In the r-ϕ-direction the corresponding numbers read 29μm and about 15μm for large pixels and strips, respectively.
Hence very similar resolutions are envisaged in either case.

3.2) Variation of pixel size
Of course the geometrical layout of the large pixel may further be optimized. For comparison also a size of $50\,\mu\mathrm{m} \times 4\,\mathrm{mm}$ instead of $100\,\mu\mathrm{m} \times 2\,\mathrm{mm}$ was chosen, keeping the total number of read-out channels constant.
The results however differ too little from those given in the previous table as to list them all. For completeness we give the resolution in the transverse momentum, see table 2.

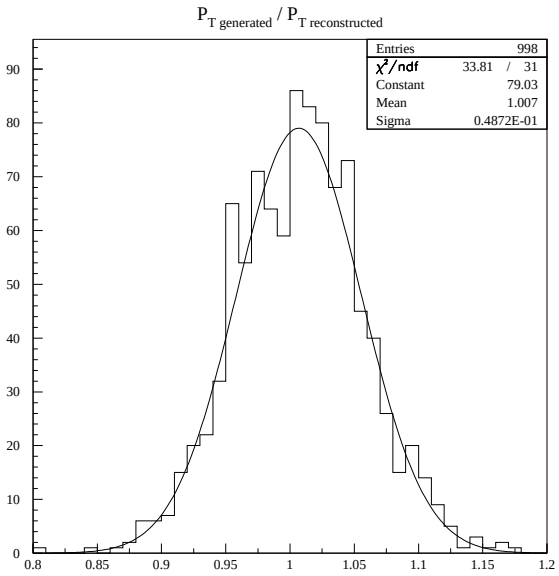

Figure 2: Ratio of reconstructed and generated transverse momentum for 100 GeV muons, using the large pixel layout.

4) Occupancy studies
One crucial issue in favour of either design is the occupancy, i.e. the number of hits per detector element per bunch crossing. During a bunch crossing, roughly 18 minimum bias events, which cannot be disentangled, are expected at the full LHC luminosity ($10^{34}\mathrm{s}^{-1}\mathrm{cm}^{-2}$). For this calculation a cross section of 70 mb and a bunch crossing rate of 40 MHz were assumed. (We shall not concern ourselves with the possibility that the full luminosity of the LHC machine will eventually be obtained at a fraction of only 73 non-empty bunches (out of 88) per turn.)

4.1) Estimations

The central density for charged tracks in so-called minimum bias events has been measured by the UA5-Collaboration at the SPS-Collider at $\sqrt{s}$ between 0.2 and 0.9 TeV[7]. Extrapolating these measurements to $\sqrt{s} = 14$ TeV a central charged track density $dn/d\eta$ of 5 to 6 seems plausible.

Hence, by purely geometrical considerations (within the specifications given above) occupancies of 2.8×10^{-5}, 1.4×10^{-3} and 2.1×10^{-5} are expected for a single large pixel element, for a single strip, and for the diamond-shaped overlapping area of two crossing strips, respectively. In these calculations we have assumed the central density to be typical for the track occupation within $\eta = \pm 1$.

Conservatively, one should increase these three numbers by a factor of 3-5 to account for charged secondaries and for low momentum curling tracks, which, due to grazing incidence, might render multiple hits in close vicinity, see below.

Furthermore, from these relatively small occupancies one may infer that the rate of double hits within 64 adjacent strips, which then would lead to ghost hits, is negligibly small.

For instance, allowing for as much as a factor of 5 in the strip occupancy (about 8×10^{-3}) the average double hit probability in a 64-strip-area is only about 0.08 per bunch crossing. (In absolute numbers: 500 of such imaginary 64-strip-areas would be populated by more than one hit in each readout cycle.)

On the other hand, these average values do not answer the question of possible *hot-spots*, i.e. chance concentrations of many hits in one detector element, either within one single physical event (mini jets, decays, etc.), or due to overlapping events within one bunch-crossing.

4.2) MC based hit multiplicities

From 180 MC generated events (based on PYTHIA[8] and DICE) i.e. corresponding to 10 individual bunch crossings, we have obtained an average occupancy of 8×10^{-3} per strip in the first X-ST layer. We include the corresponding distribution, i.e. hits per strip, see fig. 3. This sample consists of totally 5480 tracks, containing 34461 u-strip hits. Thus each track gives about 6 hits. Though the cluster width distribution, see fig. 4, peaks at only 2 hits, it extends to more than 30 hits, hence giving this surprisingly large average value (comp. sect. 4.1).

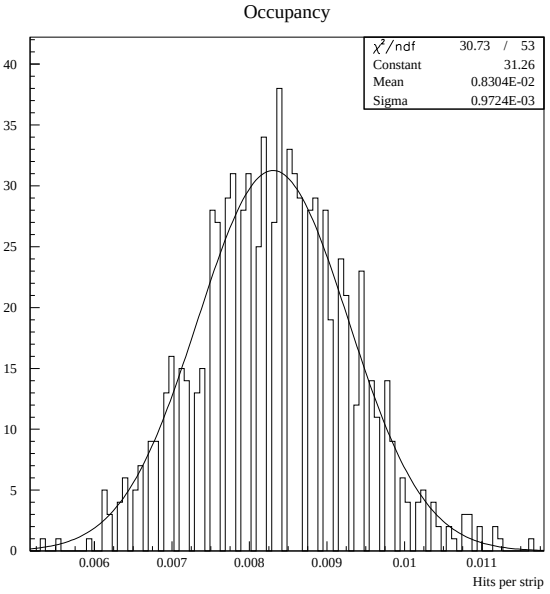

Figure 3: Hits per Strip at $r = 30\,\mathrm{cm}$.

In order to evaluate the influence of chance local concentrations of hits to the reconstruction of physics channels also non-minimum bias events are included: In accordance to the Technical Proposal[2] we assume the total $b\overline{b}$ cross section to be 500 μb, out of 70 mb for the minimum bias processes, hence the probability for exactly one $b\overline{b}$-event per bunch crossing (at full luminosity) amounts to 0.113 and the one for two such events to only 0.007.

So, for further studies it is sufficient to include *one* event of this type into each batch of 18 minimum bias events. In this way (1 $b\overline{b}$-event plus 17 overlaying minimum bias events, in each of 10 bunch crossings) the following analysis has been done, where the event sample consisted of 125 charged tracks from b-decays (rendering 623 hits in the strips).

Additionally, the effect of electronic noise in the readout channels has been simulated.

4.3) Noise
A tentative study including 10^{-3} (compare [2]) electronic noise, and, as an extreme case, also 1% electronic noise (randomly chosen, different in each bunch crossing), was performed, too. Using the occupancies determined before, the addition of such a noise increases the occupancy by a factor of 1.1 (or 2.2) in the case of strips, and by 6.6 (or by even a factor of 57) in the case of pixels - were it not for additional combinatorial background in the case of crossed strips, which roughly follows the square of the occupancy (per 64 adjacent strips). In the following we always refer to three different noise levels: No noise, 10^{-3} and 10^{-2} noise level.
We like to mention that the addition of equal amounts of electronic noise to either type of detector element neither does account for a different signal-to-noise level before irradiation, nor for the individual sensitivity to radiation damage.

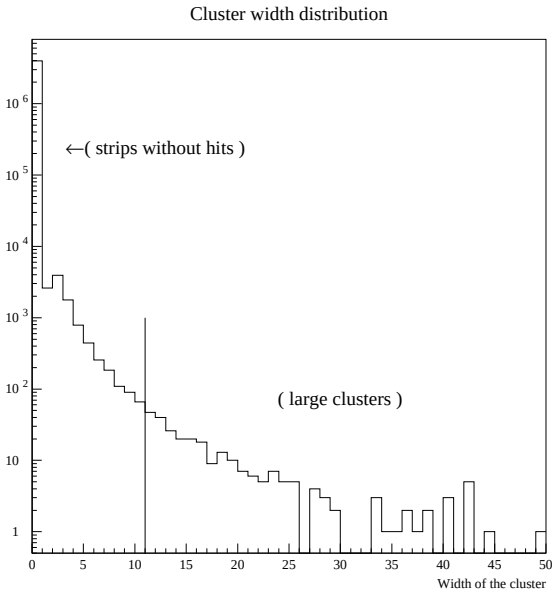

Figure 4: Distribution of cluster widths at $r = 30\,\mathrm{cm}$

4.4) Ghost hits
In order to evaluate the fraction of unresolvable tracks on account of multiple ghost hits (combinatorial background) a simple algorithm has been applied to the whole sample.
We define hits in a distance of up to 3 strips if induced by a single track as an unambiguous ("ghost free") track signal. Additionally we have required an area of 64 strips (in either direction) with respect to the position of the hit in question to be void of any other hit.
This procedure leads to a fraction of 46%, 40% or 10% (depending on the noise level provided) clean, unambiguous tracks from b-decays leaving 68, 76 or 112 tracks (containing 398, 429 or 566 hits), which deserve further treatment.

4.5) Large clusters
Single tracks may produce large clusters, compare figure 4, by which we understand sequences of hits on neighbouring strips with a length of more than 7 (or alternatively 10 , see below) strips. Typically such large clusters on the u– and on the v-strips are correlated and may easily be recognized. For instance, when there is no noise added, out of the 5480 charged tracks (including the minimum bias events) about another 100 tracks (but containing up to 10,000 hits) may be considered as ghostfree.

4.6) Unresolved ghost hits
For the remaining sample of charged tracks originating from b-decays the combinatorial background from ghost hits has been studied in detail (see table 3).
In brackets we always give the number of the corresponding hits, when a 10^{-3} or 10^{-2}, resp., random noise is superimposed. Within the acceptance of the barrel layer in question one has 125 charged tracks from b-decays. After subtraction of clean, unambiguous tracks in the sense of section 4.4., and after the large cluster recognition (see section 4.5) there remain 67 (75, 111) tracks with multiple accompanying ghost hits. These tracks, i.e. the corresponding hits, are broken down in table 3 for the various NGPH-classes (NGPH = number of ghost producing hits). The entries at NGPH = 0 are due to the fact that by the large cluster recognition process some hits (from charged b-decay tracks) have become isolated.

As a working hypothesis we assume the pattern recognition process – when using the whole inner de-

tector – will be able to cope with up to 4 NGPH (corresponding to 20 $((\mathrm{NGPH}+1)^2-(\mathrm{NGPH}+1))$ ghost hits from up to 25 combinations, including the 5 genuine hits). In order to translate the contents of table 3 into track numbers we break down those 67 (75, 111) tracks proportionally.
With this assumption one would conclude, that, given the occupancies calculated above, with the X-ST layout one might lose 15 % of the charged tracks from b-decays due to combinatorial background.
Including a 10^{-3} noise level does not change the relevant numbers, however, with a ten-fold increased noise level up to 23% of those tracks might get lost in this particular layer. (As a test of stability we quote that for a looser cut in the recognition of large clusters, see section 4.5, these figures are increased by about 0.01, whilst being less optimistic on the performance of the pattern recognition, i.e. allowing only up to 3 NGPH, the relevant figures would increase by about 0.06 .)
Clearly the LPIX layout does not suffer from such a problem.

So, including noise, a fraction of 15-23% of the charged tracks form b-decays might be lost during reconstruction. To state it the other way around: As far as pattern recognition is concerned the crossed strip layout may still function under an increased occupancy (by a factor of 2.2), caused by a 1% noise level or by even higher luminosities.

5) Conclusion and Outlook
In this article we have summarized some performance studies for two alternative layouts, namely crossed strips (X-ST) or large pixels (LPIX), at $r = 30\,\mathrm{cm}$.

Under most realistic conditions and full LHC luminosity one would expect to lose a useful space point for reconstruction for almost 16% of the charged tracks using the crossed strip layer design at $r = 30$ cm. This does not necessarily mean that those tracks are totally lost, as the outer strip layers have lower occupancies, and do not generally have too many ghost hits for just the same tracks.
A pixel layer at $r = 30$ cm would ease pattern recognition in the barrel, as the pixels give real space points.

Of course further detailed studies have to be devised, but are beyond the scope of this article.
We have not considered the question, whether (once one demands these space points) a location at $r = 30$ cm, appears – for reasons of radiation hardness – the innermost possible location for such a detector element (as pixel elements are also foreseen at $r = 11.5$ and 16.5 cm).
Furthermore, questions like radiation hardness in general, signal-to-noise ratio, necessity for fully depleted operation, possible cross talk and other specific problems in either detector design have not been addressed in this study.

Acknowledgements
We are grateful for fruitful discussions to K.H. Becks, C. Gößling, A. Poppleton and N. Wermes.

References

[1] ATLAS Letter of Intent, CERN/LHCC 92-4.

[2] ATLAS Technical Proposal, CERN/LHCC 94-43, ISBN 92-9083-067-0.

[3] SLUG-Manual, R.S. DeWolf and S.W. O'Neale, ATLAS-SOFT-NO-12.

[4] DICE-Manual, ATLAS-SOFT-NO-11.

[5] iPatRec-Manual, R. Clifft and A. Poppleton.

[6] Implementation of Large Pixel Detectors in SLUG/DICE, P. Luthaus et al., ATLAS-SOFT-NO-19.

[7] G.J. Alner et al., Zeit. Phys. C33 (1986),1; C. Geich-Gimbel, Int. J. Mod. Phys. A4 (1989),1527.

[8] T. Sjöstrand, CERN-TH.6488/92.

[9] ATRECON-Manual, ATLAS-SOFT-NO-15.

Table 1: Single track parameter resolution. The first line in the table always corresponds to the strip option (X-ST), the second one to just one layer of large pixels (LPIX).

Electrons: momentum	10	50	100	500	GeV
$\Delta\phi$	.215	.111	.096	.093	mrad
	.221	.117	.108	.099	mrad
$\Delta\theta$	.641	.552	.539	.504	mrad
	.731	.573	.568	.506	mrad
$\Delta\eta$	.659	.571	.557	.460	$\times 10^{-3}$
	.736	.586	.591	.518	$\times 10^{-3}$
p_T	.018	.033	.051	.234	
(ratio)	.022	.034	.057	.224	

Muons: momentum	10	50	100	500	GeV
$\Delta\phi$	.191	.097	.092	.087	mrad
	.178	.106	.097	.095	mrad
$\Delta\theta$	.637	.535	.511	.512	mrad
	.672	.536	.538	.551	mrad
$\Delta\eta$	.626	.554	.537	.546	$\times 10^{-3}$
	.697	.542	.558	.577	$\times 10^{-3}$
p_T	.014	.027	.049	.227	
(ratio)	.015	.029	.049	.232	

Table 2: Single track parameter resolution. The first line in the table always corresponds to the strip option (X-ST), the second one to just one layer of large pixels (LPIX) of $50\,\mu\text{m} \times 4\,\text{mm}$ size.

Electrons: momentum	10	50	100	500	GeV
p_T	.018	.033	.051	.234	
(ratio)	.021	.032	.054	.228	

Muons: momentum	10	50	100	500	GeV
p_T	.014	.027	.049	.227	
(ratio)	.017	.029	.049	.216	

Table 3: Number of accompanying, ghost producing hits "NGPH". In brackets we give the corresponding numbers for 10^{-3} and 10^{-2} noise level.

NGPH	Hits from b-decays
0	6 (4, 0)
1	55 (77, 87)
2	56 (61, 95)
3	34 (38, 62)
4	31 (32, 60)
5	8 (9, 30)
6	3 (3, 10)
7	5 (4, 8)
8	0 (1, 2)
9	0 (0, 4)
> 9	55 (55, 55)